AJS
Algerian Journal of Sciences
Volume 2 – Issue 1 – PP. 50 – 62

Chemical Bonding in CuAlX2 with X= S, Se and Te Chalcopyrites based on Structural Elastic and Electronic Properties

Y. Medkour[1,2*], F. Djeghloul [2, 3], S. Kheloufi[1,2], A. Saoudi [1,4], M. Reffas [1,4], K. Haddadi [1,4] and A. S. Messalti [1,4]

[1] Department of Physics, Faculty of Sciences, University of Setif1, 19000 Setif, Algeria

[2] Laboratoire d'Etudes des Surfaces et Interfaces des Matériaux Solides (LESIMS), Université de Setif1, 19000, Setif, Algérie.

[3] Department of Basic Education in Technology, Ferhat ABBAS University Setif 1, Setif, Algeria
[4] Emergent Materials Research Unit (EMRU), University Ferhat Abbas Setif 1, 19000, Setif, Algeria

Abstract

We report results of first principal calculations of the electronic, structural and elastic properties of $CuAlX_2$ (X=S, Se and Te) chalcopyrites. Up to 10 GPa, the pressure effect on the lattice parameters (a, c and v) is discussed, the linear compressibility of *a*, *c* axes and the bond strength between the nearest neighbors of Al-X and Cu-X are studied. Elastic constants C_{ij} for single crystal; the deduced parameters bulk modulus *B*, shear modulus *G*, Young modulus *E* and the compressibility coefficients χ_a, χ_c, χ_v for polycrystalline aggregate are presented. Bonding nature and bonds strength are discussed based on two points of view. Firstly, from the pressure effect on the structural parameters and the relative change of the bonds length. Secondly, from the electronic aspect based on the partial densities of states and the electronic charge distribution.

Keywords: Chalcopyrites, Chemical bonding, Structural properties, Elastic moduli.

Article History

Received: 24-12-2025
Accept: 15-05-2025
Published: 30-09-2025

* Corresponding author Email
(you_med2000@univ-setif.dz)

1 Introduction

Chalcopyrite materials have been the subject of numerous works around the world [1-13]. They have been used in various industrial applications, such as optical device, photovoltaic optical detectors, light emitting diodes and non linear optics [1-13], Cu- chalcopyrite absorbers represent the most advanced thin film technology [11]. The electronic properties of CuAlX2 compounds, with X=S, Se and Te, are extensively studied by means of experimental and theoretical methods showing a direct band gap which decreases in the sequence 3.49, 2.67 and 2.06 eV for CuAlS2, CuAlSe2 and CuAlTe2 respectively [13]. It is well known that, the energy gap is generally underestimated by first principle methods [14], the results reported by Reshak et al. [15] are among the best available theoretical data for the band gap of these compounds [16-18]. Under pressure effect, CuAlS2 remains stable up to 14.8 GPa and no phase transition is observed, however a phase transition occurs for CuAlSe2 from the body centered tetragonal (BCT) to rocksalt (NaCl) type structure at about 12.5 GPa [19]. Abdellaoui et al. [16] using FP-LMTO approaches studied the structural, elastic and electronic properties of CuAlS2, CuAlSe2 and CuAlTe2. They predicted a phase transition from the BCT to rocksalt type structure (NaCl) at 13.55, 8.89 and 5.58 GPa for CuAlS2, CuAlSe2 and CuAlTe2 respectively. Pressure effect on elastic constants Cij of CuAlSe2 and CuInSe2 is studied by Gürel et al. [20]. C11, C33, C13 and C12 showed a linear increase with pressure, however C66 and C44 decrease nonlinearly with increasing pressure, their results are in good agreement with the only available experimental elastic constants for CuInSe2 at 0 GPa [21]. Recently electronic and optical properties of CuATe2 (A=Al, Ga and In) have been studied [22], their results show that CuGaTe2 and CuInTe2 are promising materials for photovoltaic applications.

Despite of the mentioned works on $CuAX_2$ (A= Al, Ga, In. X=S, Se and Te) compounds and their importance for various applications, we are interesting to $CuAlX_2$ (X=S, Se and Te) compounds at the BCT phase, which are stable up to about 10 GPa [19]. The purpose of this work is to present a deeper analysis of the structural properties, the compression behavior, the elastic properties under pressure. The bonding mechanism in these compounds was delighted.

Authors may submit only papers that have not been published before and have been read and approved by all authors. The manuscript should not be submitted anywhere else while under consideration. The font for Body Text should be Times New Roman 12 pts. All papers should be limited to 7-12 pages.

2 Calculation Details

CASTEP (Cambridge Serial Total Energy Package) code [23] is used to perform this study. The problem of fundamental eigenvalue is resolved using the density functional theory [24] and the Kohn-Sham approach [25]. In order to reduce the very important number of plane wave (PW), that's describe the electron's function, a fictive potential (pseudopotential) is generated to replace the real atomic potential [26]. By the use of the pseudopotential approach, the number of plane waves needed to describe all atomic electrons is decreased to a limit number of valence electrons. Pseudo atomic calculations are performed with; Cu: $3d^{10}4s^{1}$, Al: $3s^{2}3p^{1}$, S: $3s^{2}3p^{4}$ Se: $4s^{2}4p^{4}$ and Te: $5s^{2}5p^{4}$. Local density approximation LDA with the CA-PZ functional [27] is used to calculate the exchange correlation energy. The Broyden- Fletcher- Goldfarb- Shanno (BFGS) algorithm [28,29] is used to find the fundamental energy of the crystal. After careful convergence tests, we used 5×5×3 irreducible k points to sampling the first Brillouin zone [30] and a cut off energy $E_{cut\ off}$ = 350 eV for an ultra-soft pseudopotential [26].

Calculations are done since the energy tolerance is about to 5.10^{-6} eV/atom, the maximum force is equal 0.01 eV/ Å, the maximum stress is lower than 0.02 GPa and a maximum displacement doesn't exceed 5.10^{-4}Å.

3 Results and Discussion

3.1 Structural Properties

In order to reach the ground state, we calculated the total energy of the body centered tetragonal (*BCT*) at various volumes compared to the experimental one. The data, as presented in Fig.1, are fitted to the third order Birch-Murnaghan equation of state (EOS) [31], the output results are summarized in Table1, together with the available experimental [12, 32] and theoretical [16,17] data.

Table 1 : Summary of calculated lattice parameters, bulk modulus *B* and its pressure derivative *B'*, with the available experimental and theoretical data.

Compd.	Method	*a (Å)*	*c (Å)*	*v (Å)*^{3}	*c/a*	*u*	*B** *(GPa)*	*B'*
	Our calc.	**5.179**	**10.352**	**277.70**	**1.998**	**0.250**	**99.6**	**4.5**
	Exp.	5.310[32]	10.420[32]	293.80[32]	1.962[32]	0.27[32]	94[33], 99±3[34]	4[34]
$CuAlS_2$	Calc. [16]	5.18	10.35	—	—	0.25	100.0	4.12
	Calc. [17]	5.313	10.429	294.39	1.963	—	82.35	—
	Our calc.	**5.472**	**10.900**	**326.47**	**1.991**	**0.245**	**80.9**	**4.6**
$CuAlSe_2$	Exp.	5.606[32]	10.900[32]	342.55[32]	1.954[32]	0.26[32]	85±8 [19]	4.6[19]
	Calc. [16]	5.47	10.9	—	—	0.245	76.0	3.82
	Calc. [17]	5.609	10.957	344.72	1.953	—	71.15	—
	Our calc.	**5.932**	**11.823**	**416.03**	**1.993**	**0.237**	**63.4**	**4.7**
$CuAlTe_2$	Exp.[32]	5.964	11.780	419.00	1.975	—	—	—
	Calc. [17]	6.061	11.973	439.83	1.975	—	52.72	—
	Calc. [16]	5.94	11.83	—	—	0.236	57.6	4.26

* Calculated from the EOS.

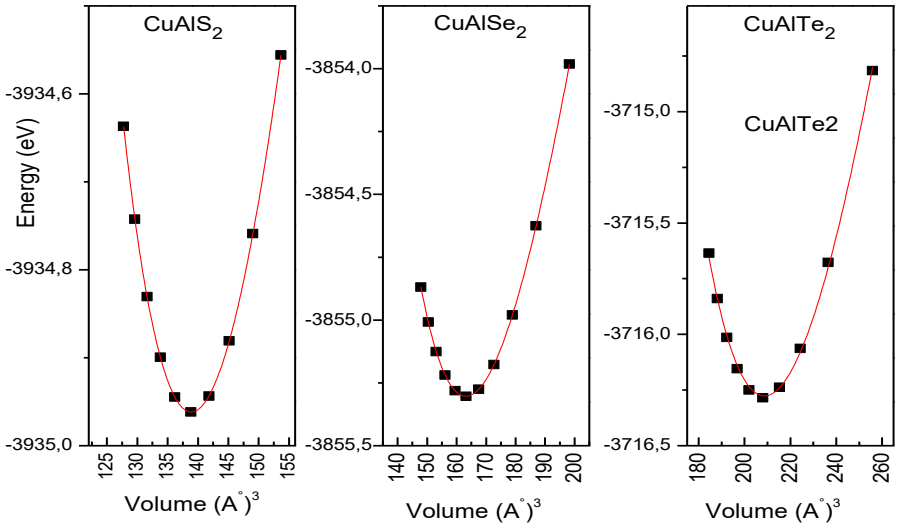


Figure 1: Total energy versus volume for $CuAlS_2$, $CuAlSe_2$ and $CuAlTe_2$.

The obtained results for the lattice parameters *a* and *c* are in good agreement with the experimental results. The deviation from experimental values is less than 2.5 %, however the equilibrium volumes are underestimated by about 5.4, 4.6 and 0.7% for $CuAlS_2$, $CuAlSe_2$ and $CuAlTe_2$ respectively. One can observe that the substitution of S by Se (Se by Te) atoms enhanced the equilibrium volume by about 18% (27%). This increase is in correlation with the increasing atomic radius of S, Se and Te atoms. The disagreement between the calculated values of the ratio c/a and the experimental ones is within 2%. Calculated bulk moduli B from the EOS are 99.6, 80.9 and 63.4 GPa for $CuAlS_2$, $CuAlSe_2$ and $CuAlTe_2$ respectively, they have the same trend as the equilibrium volume, satisfying the well known relation $B\sim(1/v)$ [35]. The bulk moduli of $CuAlS_2$ and $CuAlSe_2$ are in good agreement with the experimental ones, within a deviation of 5% [19, 33, 34]. However, in our knowledge, there is no experimental data of the bulk modulus for $CuAlTe_2$. Then our calculated bulk moduli are improved than previous theoretical data [16, 17]. The internal parameters *u* of S, Se and Te are in agreement with those reported in references [16, 32].

The pressure effect on the equilibrium volume of $CuAlS_2$, $CuAlSe_2$ and $CuAlTe_2$ is presented in Fig.2. At a pressure of 10 GPa, the contraction of the volume increases as 8, 9.4 and 11.3% for $CuAlS_2$, $CuAlSe_2$ and $CuAlTe_2$ respectively, which is in accord with the variation of the calculated bulk moduli of these compounds as shown in tables 1 and 3. The observed disagreement between the experimental and theoretical curves in Fig.2 could be explained by the use of LDA approximation which is well-known to underestimate the equilibrium volume [24].

Since these compounds crystallize in the tetragonal symmetry (i.e. $a=b\neq c$), it is interesting to examine the response of the principal crystallographic directions along *a* and *c* axes against increasing pressure, our results are shown in Fig.3. The contraction of *a* axis (2.9%) is more important than that of *c* axis (2.5%) for $CuAlS_2$. For $CuAlSe_2$ the contraction increases in the same trend, along *a* axis is about 3.3% and for *c* axis is 3.1%. However, for $CuAlTe_2$ the contraction in both direction *a* and *c* axes is almost identical (3.9%).

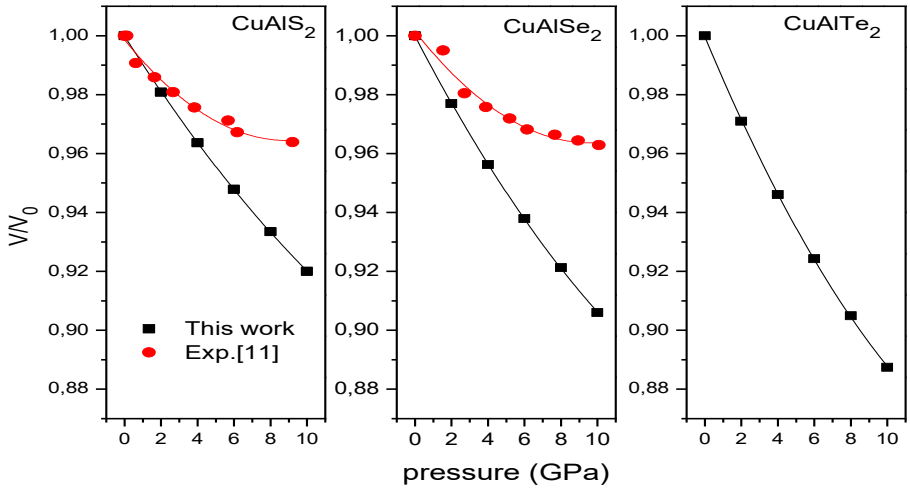


Figure 2: Relative volume change versus pressure for $CuAlS_2$, $CuAlSe_2$ and $CuAlTe_2$.

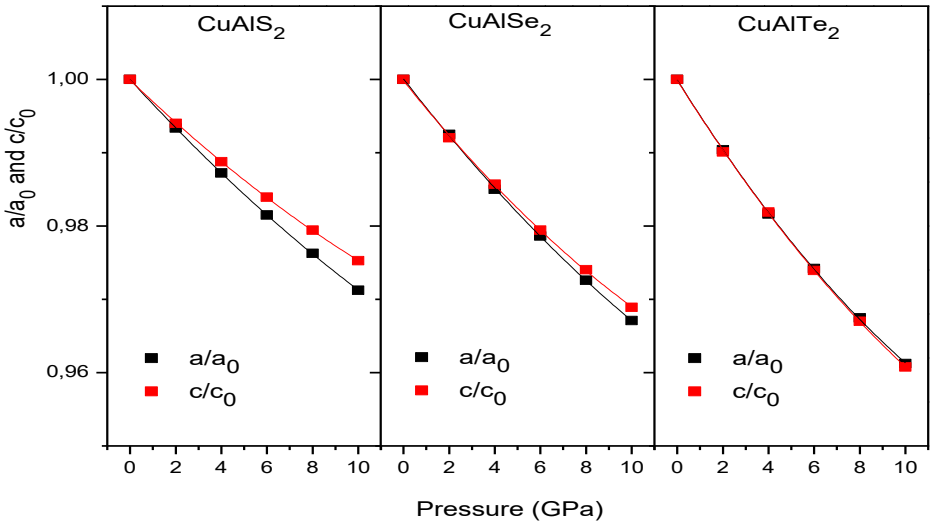


Figure 3: Relative change of lattice parameters *a* and *c* versus pressure, for $CuAlS_2$, $CuAlSe_2$ and $CuAlTe_2$.

On the other side, the contraction of *a* and *c* directions could be useful to discuss the strength of both directions. Firstly, for each separate compound, we observe for $CuAlS_2$ and $CuAlSe_2$ that the *c* direction is more resistant to contraction, and then it is stronger than *a* direction. Nevertheless, the strength of the two directions *a* and *c* is almost identical for $CuAlTe_2$. Secondly, for all understudy compounds, we observe a decrease of the strength of *a* and *c* directions as the sequence $CuAlS_2$, $CuAlSe_2$ and $CuAlTe_2$. These results are in agreement with the higher resistant of $CuAlS_2$ to volume change under pressure. Since there are no previous experimental or theoretical studies on the strength of these compounds, this inspires us to investigate the relative bond length up to 10 GPa, as presented in Fig.4. The X—Al bonds are stiffer than X—Cu bonds (X=S, Se), the strength of Te—Al and Te—Cu bonds is almost identical. The stiffness of the bonds X—Al and X—Cu decreases from $CuAlS_2$, $CuAlSe_2$ and CuAlTe.

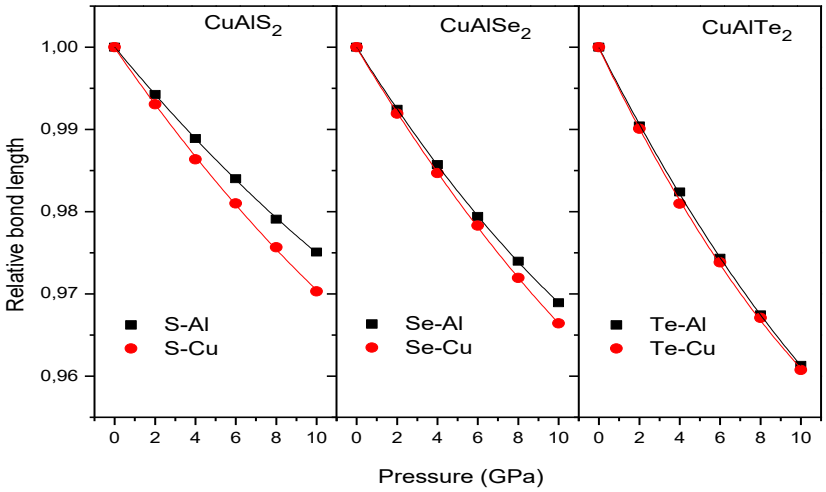


Figure 4: Relative change of the bond length X—Al and X—Cu versus pressure, for $CuAlS_2$, $CuAlSe_2$ and $CuAlTe_2$.

3.2 Elastic Properties

Results of elastic constants C_{ij} are carried out according to the finite elastic strain technique [31, 36]. Elastic properties of a tetragonal crystal can be described using six independent elastic constants [37] C_{11}, C_{33}, C_{44}, C_{66}, C_{12} and C_{13}. Our results for C_{ij} are summarised in Table 2 with previous calculated data. The requirements for mechanical stability of the tetragonal system are [38]: $C_{11}>0$, $C_{33}>0$, $C_{44}>0$, $C_{66}>0$, $C_{11}-C_{12}>0$, $(C_{11}+C_{33}-2C_{13})>0$ and $[2(C_{11}+C_{12})+C_{33}+4C_{13}]>0$, these conditions are satisfied by the values reported in Table 2. This ensures again the stability of the previously synthesized compounds. Our results are in good agreement with those reported in [16, 17]. C_{11} is related to the unidirectional compression along *a* or *b* axes, while C_{33} is related to *c* direction [37]. At 0 GPa, we observe that C_{33} is more important than C_{11} for $CuAlS_2$ and $CuAlSe_2$, while for $CuAlTe_2$ C_{11} turns to be slightly higher than C_{33}. Going from $CuAlS_2$ to $CuAlSe_2$, C_{ij} constants decrease at least by about 17%, while they decrease at least by about 18% if we substitute Se by Te. As shown in Fig.5, with increasing pressure up to 10 GPa, C_{11}, C_{33}, C_{12} and C_{13} increase linearly with pressure [20], while C_{44} and C_{66} decrease slightly. These results are in good agreement with those reported for the contraction of *a* and *c* directions as discussed in section 3.1.

Table 2 : Summary of calculated single crystal elastic moduli *Cij* in GPa.

Compd.		C_{11}	C_{33}	C_{44}	C_{66}	C_{12}	C_{13}
$CuAlS_2$	Our calc.	**131.9**	**135.9**	**58.03**	**55.4**	**80.6**	**83.8**
	Calc. [16]	133.0	135.0	56.5	53.7	80.7	84.5
	Calc. [39]	91.7	105.8	38.8	35.3	57.3	67
$CuAlSe_2$	Our calc.	**108.8**	**110.4**	**46.6**	**45.8**	**66.2**	**68.1**
	Calc. [16]	102.9	106.0	46.0	42.9	60.9	62.7
	Calc. [20]	102.9	104.5	42.8	41.5	63.4	65.7
	Calc.[39]	86.8	100.2	36.7	33.4	54.3	63.5

$CuAlTe_2$	Our calc.	**87.7**	**87.2**	**38.2**	**37.6**	**50.8**	**51.5**
	Calc. [16]	81.1	87.7	39.3	36.1	44.7	45.1
	Calc. [39]	83.1	95.9	35.2	32	51.9	60.8

Polycrystalline elastic constants are presented using only the Hill's assumption, which is defined as the arithmetic average of the Voigt and Reuss approximations [37]. The bulk modulus B gives information about materials resistance to volume changes. However, shear modulus G provides information on the shape change [37]. Our results for the bulk modulus B, shear modulus G, Young's modulus E and the compressibility coefficients χ_a, χ_c, χ_v are summarized in Table 3.

Table 3: Summary of calculated polycrystalline elastic constants.

Compd.		B^* (GPa)	G(GPa)	E(GPa)	χ_a $(TPa)^{-1}$	χ_c $(TPa)^{-1}$	χ_v $(TPa)^{-1}$
$CuAlS_2$	Our calc.	**99.7**	**41.1**	**108.6**	**3.5**	**3.02**	**10.04**
	Calc. [16]		40.4	106.9			
$CuAlSe_2$	Our calc.	**81.1**	**33.8**	**88.84**	**4.2**	**3.8**	**12.2**
	Calc.		32.9 [16]	86.2 [16]	4.4 [20]	4.0 [20]	
$CuAlTe_2$	Our calc.	**63.7**	**27.5**	**69.5**	**5.2**	**5.2**	**15.8**
	Calc. [16]		28.9	74.4			

* Calculated from C_{ij} constants.

Calculated bulk moduli from elastic constants C_{ij} are slightly higher than those calculated from the EOS, the bulk modulus decreases in the sequence $CuAlS_2$, $CuAlSe_2$ and $CuAlTe_2$. Bulk moduli B are about 57% higher than the corresponding shear moduli G, which reflects the weak resistance to shear deformation in these compounds, also shear modulus decreases in the same trend as the bulk modulus. Substitution of S by Se (Se by Te) atoms decreases the Young modulus E by 18% (21%). From Fig.6, we observe a linear increase of the bulk modulus with pressure. However, shear and Young moduli decrease slightly with increasing pressure. We can conclude that increasing pressure reduces the resistance of these compounds to shear deformations.

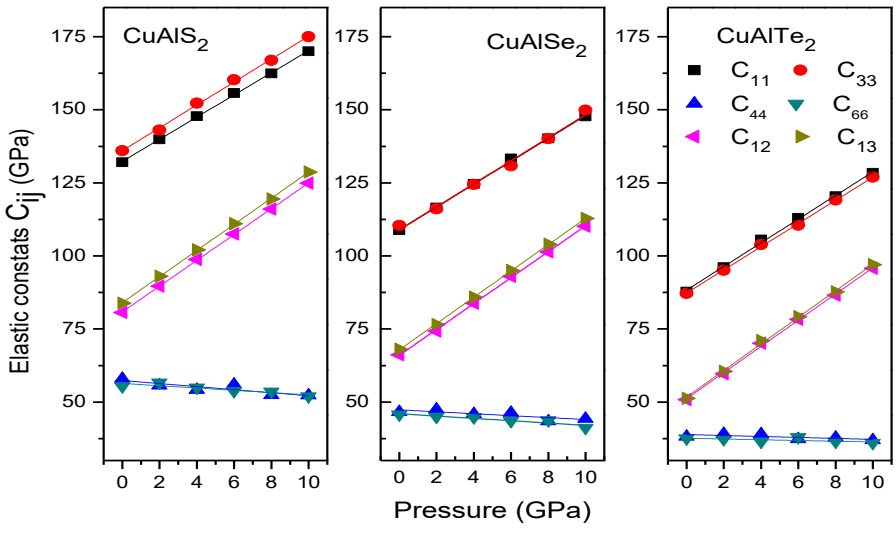


Figure 5: Elastic constants versus pressure, for $CuAlS_2$, $CuAlSe_2$ and $CuAlTe_2$.

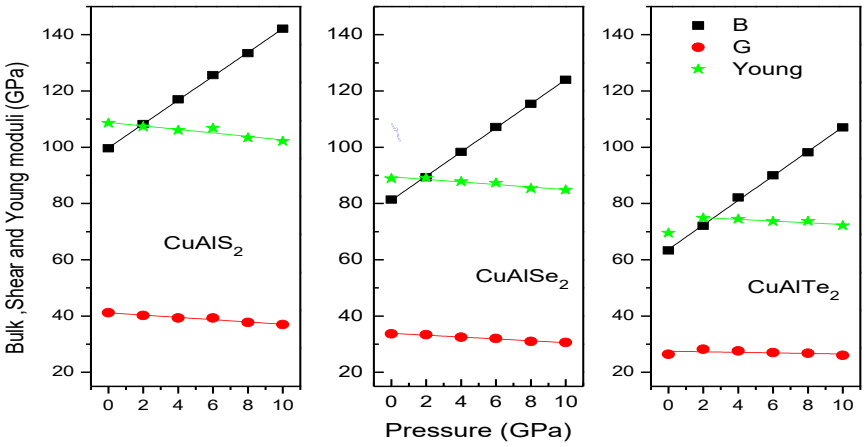


Figure 6: Polycrystalline elastic constants versus pressure, for $CuAlS_2$, $CuAlSe_2$ and $CuAlTe_2$.

The estimated compressibility coefficients χ_a, χ_c and χ_v [20] are listed in Table 3. As stated above, the linear compressibility along *a* direction is more important than along *c* direction for $CuAlS_2$, $CuAlSe_2$, nevertheless, the χ_a and χ_c of $CuAlTe_2$ are identical. The volume compressibility χ_v increases in the sequence $CuAlS_2$, $CuAlSe_2$ and $CuAlTe_2$. Note that our calculated values for CuAlTe2 are in agreement with those reported by Gürel *et al.* [20], with a deviation less than 5%. Increasing pressure leads to reduce the compressibility of these compounds as shown in Fig.7.

3.3 Electronic Properties and Chemical Bonding

To give a detailed analysis of the structural and elastic behavior of these compounds, we have improved our study by investigating the electronic properties and the chemical bonding in these compounds. Partial densities of state (PDOS) is a powerful tool for discuss the nature of bonds and their origins [40]. In Fig.8, we have presented the densities of states by orbital and by atoms which are found similar to those reported earlier [16-18]. The valence band, below the Fermi level, is constructed from three parts:

i- The lower parts originate from X-s electrons (with X= S, Se and Te) and Al-(s, p) electrons.

ii- The middle parts extend from -8 to -2.4 eV for $CuAlS_2$, from -7 up to -3.3 eV for $CuAlSe_2$, and from -6.5 eV till -2.4 eV for $CuAlTe_2$. These regions come from Cu-d, X-p and Al-(s, p) electrons.

iii- The higher parts starting from -3.3, -2.6, -2.4 eV up to Fermi level for $CuAlS_2$, $CuAlSe_2$ and $CuAlTe_2$ respectively. These sections originate from Cu-d, X-p and Al-p electrons. One can observe a decrease of the band gap energy between the middle and the upper part for $CuAlS_2$, $CuAlSe_2$, and then it disappears for $CuAlTe_2$.

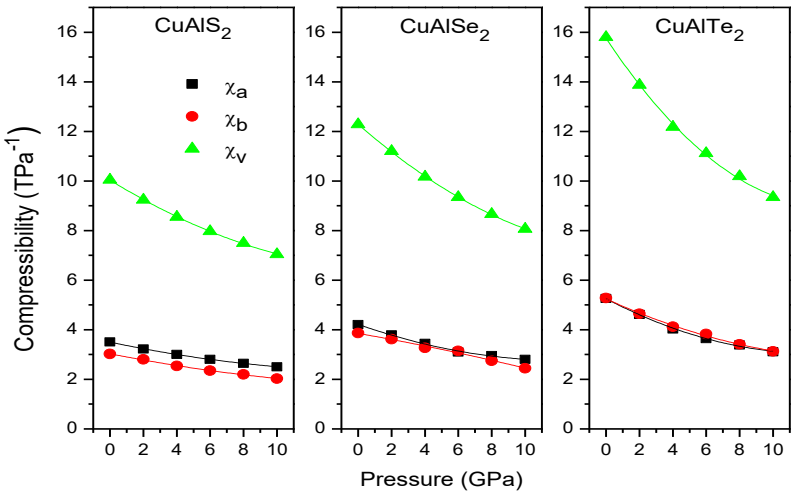


Figure (7): Compressibility coefficients versus pressure, for $CuAlS_2$, $CuAlSe_2$ and $CuAlTe_2$.

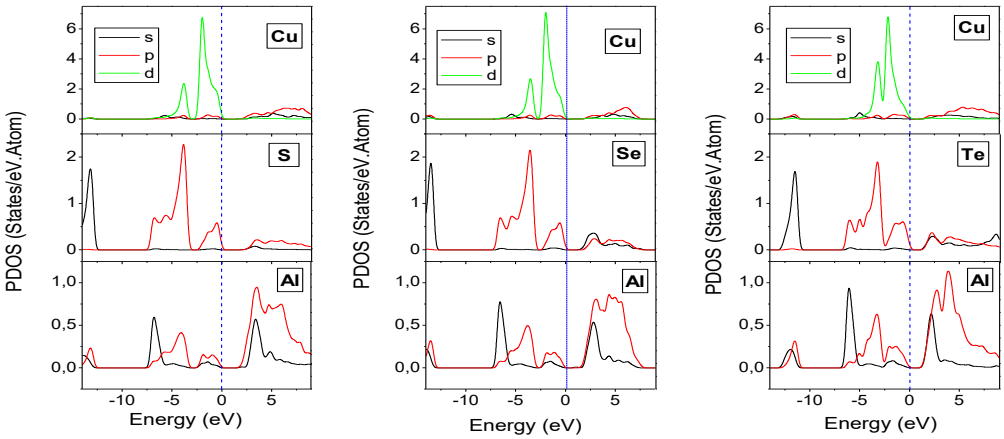


Figure (8): Calculated partial densities of states for $CuAlS_2$, $CuAlSe_2$ and $CuAlTe_2$. Fermi level is set at 0 eV

The conduction band beyond the Fermi level is constructed from Cu-(s, p), X-(s, p), and Al-(s, p) states.

Based on the partial densities of states, Fig.8, we observe at lower energy a strong hybridization X-s—Al-(s, p). At about -6.4 eV, X-p states are hybridized with Al-s. X-s states are hybridized with both Cu-d and Al-p states at the energy level extending from -3.5 eV till the Fermi level.

To provide a deeper study on the bonding properties, we have calculated the overlap population for nearest neighbors in the crystal (Table 4). Positive values express bonding states between atoms, while negative values show antibonding states [41, 42]. The present calculations display a positive overlapping population between X—Cu and X—Al bonds (with X= S, Se and Te), then the present bonds are in bonding state. Moreover, the high overlap value, the high degree of covalency in the bond [41] and according to the values reported in Table 4, X—Al bonds are stronger than X—Cu bonds. On the other side, the difference in electronegativity between X, Cu and Al atoms gives rise to a charge transfer then ionic bonds will be occurred. Significant charge transfer between S and Al atoms leads to a strong ionic bonding in $CuAlS_2$. For $CuAlSe_2$, the charge transfer is reduced, and then the ionic bonding is weakened.

In the case of $CuAlTe_2$, an important charge transfer from Te towards Cu atoms generates a strong ionic bonding between Te and Cu atoms. Strengthen of Te—Cu bonds and weakens of Te—Al bonds give us a good explanation of the presented results in Figures 3, 4 and ~~7~~ 5. Our results are in good agreement with those reported by Ouahrani *et al.* [43].

Table 4: Bond length and overlap population for nearest neighbors in $CuAlS_2$, $CuAlSe_2$ and $CuAlTe_2$.

Compounds	*Bonds*	*Bond length (Å)*	*Bond population (|e|)*	*Anion and cation charge (|e|)*
$CuAlS_2$	S— Al S— Cu	2.24189 2.24258	0.58 0.34	Cu: 0.09 Al: 0.84 S: -0.47
$CuAlSe_2$	Se— Al Se— Cu	2.38088 2.35232	0.55 0.33	Cu: -0.38 Al: 0.45 Se: -0.04
$CuAlTe_2$	Te— Al Te— Cu	2.61131 2.52159	0.59 0.46	Cu: -0.64 Al: 0.11 Te: 0.26

We have extended our investigation of the chemical bonding to the charge density distribution in these compounds, valence charge density maps are illustrated in Fig.9, these results are referred to (110) plane. strong directional charge distribution along X—Cu and X—Al directions is observed, the electrons are shared between X—Cu and X—Al atoms, which is a characteristic of the covalent bonds, a deeper look on these maps shows a decrease of the bond strength from $CuAlS_2$ to $CuAlTe_2$. Moreover, the covalency decreases in the same trend as the electronegativity in the order S, Se and Te [40], which reduces the interstitial charge as shown in Fig.9.

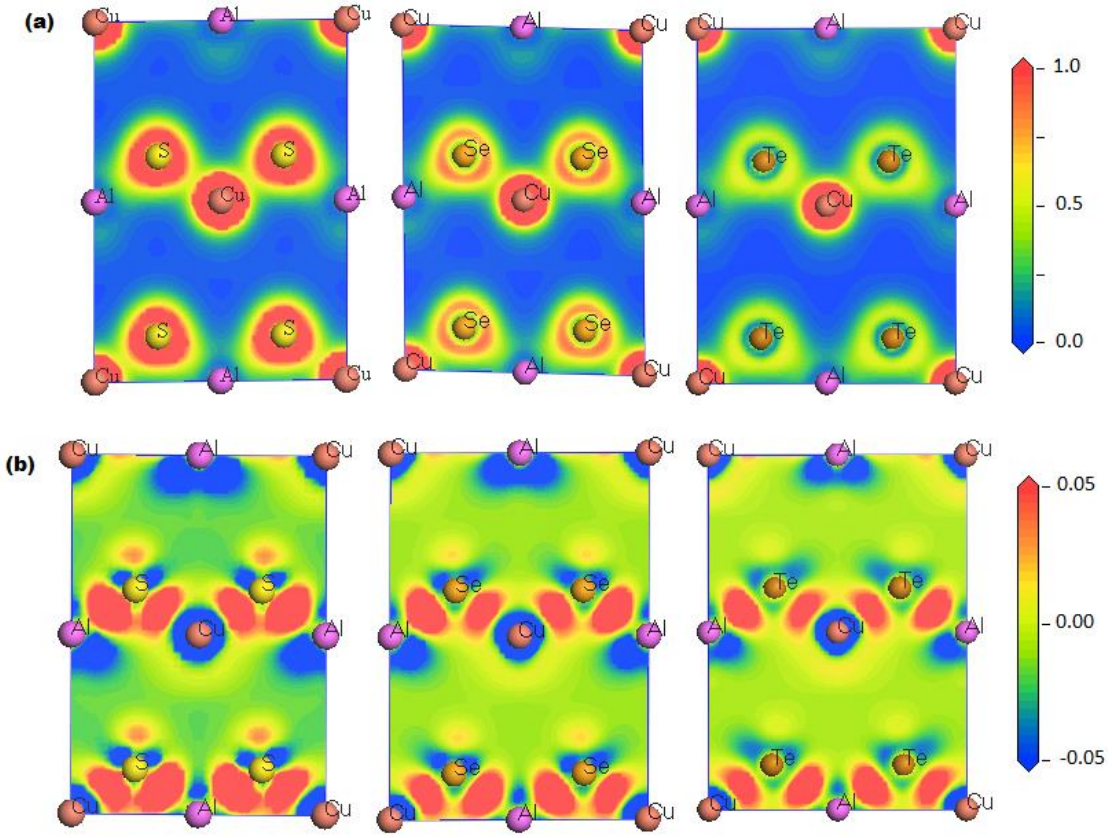


Figure (9): Calculated valence charge density for $CuAlS_2$, $CuAlSe_2$ and $CuAlTe_2$.

3 Conclusion

Based on first principal calculations, we have presented a study of structural properties up to 10 GPa. The calculated lattice parameters, bulk modulus and its pressure derivative are in agreement with previous experimental and theoretical data. The bulk modulus decreases as the sequence $CuAlS_2$, $CuAlSe_2$ and $CuAlTe_2$. Elastic constant of single crystal C_{ij} are in satisfactory with the available theoretical data, the pressure effect on the unidirectional elastic moduli C_{11} along *a* direction, and C_{33} along *c* direction are in good agreement with the results obtained for a/a_0 and c/c_0 respectively. Also, polycrystalline elastic constants are reported. Based on the pressure effect, we showed that *c* direction is stronger than *a* direction for $CuAlS_2$ and $CuAlSe_2$, however for $CuAlTe_2$ the strength of both directions *a* and *c* is almost identical. Moreover, the relative bond length against increasing pressure shows that X-Al bonds are stiffer than X-Cu bonds for $CuAlS_2$ and $CuAlSe_2$, while Te-Al and Te-Cu bonds have the same strength. We observed a weakening of both bonds X-Al and X-Cu in the sequence $CuAlS_2$, $CuAlSe_2$ and $CuAlTe_2$. To provide additionally data on the bonding mechanism in these compounds, we presented the partial densities of states. The results show different hybridizations between X-s —Al-(s, p) at about -13 eV, X-p—Cu-d and X-p — Al-p from -3.5 eV till Fermi level. From Mulliken analysis of the overlap population, the present bonds in these compounds are of covalent type. Further investigations of the valence charge density confirm the predominance of the covalent bonds, with a signature of ionic bonds. The bonds covalency decreases with the electronegativity of S, Se and Te atoms.

References

[1] A. H. Reshak, Physica B **369**, 243(2005).

[2] A. H. Reshak, V. V. Atuchin, S. Auluck and I. V. Kityk, J. Phys. Condens. Matter **20**, 325234 (2008).

[3] A. H. Reshak, S. Auluck, I. V. Kityk, A. Perona and B. Claudet, J. Phys.: Condens. Matter **20**, 325213 (2008).

[4] A. H. Reshak and S. Auluck, PMC Physics B (2008) 1:12

[5] T. Ouahrani, A. H. Reshak, R. Khenata, B. Amrani, M. Mebrouki, A. Otero-de-la-Roza, V. Luaña. J. Solid State Chem. **183**, 46 (2010).

[6] H. S. Saini, M. Singh, A. H. Reshak, M. K. Kashyap, J. Alloys Compd **518**, 74 (2012).

[7] N. Seddiki, T. Ouahrani, B. Lasri, T. Benouaz, A. H. Reshak, B. Bouhafs, Mater. Sci. . Semi. Proc., **16**, 1454 (2013).

[8] A. H. Reshak, *Advences in Condensed Matter Physics*, Signpost. India 2009.

[9] A. Jager-Waldau, Solar Energy Mater. & Solar Cells **95,** 1509 (2011).

[10] B. Pamplin, Prog. Crystal Grouth Charact., **1,** 331 (1978).

[11] S. Siebentritt and U. Rau, *Cu-Chalcopyrites – Unique Materials for Thin-Film Solar Cells* in wide-gap chalcopyrites. Eds. S. Siebentritt and U. Rau, Springer, 2005.

[12] A. Shaukat, R. D. Singh, J. Phys. Chem. Solids, **39**, 1269 (1978).

[13] A. Zunger, Appl. Phys. Lett., 50 (1987) 164-166.

[14] David S. Sholl and Jan Steckel, *Density functional theory: a practical introduction*. John Wiley & Sons, 2009.

[15] A.H. Reshak, S. Auluk, Solid State Commun., **145**, 571 (2008) -576.

[16] A. Abdellaoui, M. Ghaffour, M. Bouslama, S. Benalia, A. Ouerdane, B. Abidri, Y. Monteil, J. Alloys and Compd., **487**, 206 (2009).

[17] V. Jayalakshmi, S. Davapriya, R. Murugan, B. Palanivel, J. Phys. Chem. Solids, **67**, 669 (2006).

[18] U.P. Verma, Per Jensen, M. Sharm, P. Singh, Comp. Theo. Chem., 975, 122 (2011).

[19] R. S. Kumar, A. Sekar, N. Victor Jaya, S. Natarajan, S. Chichibu, J, Alloys Compod., **312**, 4 (2000).

[20] T. Gürel and R. Eryigit, J. Phys.: Condens. Matter, 18, 1413 (2006).

[21] R. Fouret, B. Hennion, J. Gonzalez and S. M. Wasim, Phys. Rev., B, **47**, 8269 (1993).

[22] Zhang Xian-Zhou, Shen Ke-Sheng, Jiao Zhao-Yong, Huang Xiao-Fen, Comp. Theo. Chem., **1010**, 67 (2013).

[23] M. D. Segall, P. J. D Lindan, M. J. Probert, C. J. Pickard, P. J. Hasnip, S. J. Clark and M. C. Payne, J. Phys : Condens. Matter, **14**, 2717 (2002).

[24] J. Kohanoff, *Electronic structure calculations for solids and molecules*, Cambridge University Press, 2006.

[25] W. Kohn, L. J. Sham, Phys. Rev. A **140**, 1133 (1965).

[26] M. C. Payne, M. P. Teter, D. C. Allan, T. A. Arias and J. D. J. Joannopoulos, Rev. Mod. Phys., **64**, 1045 (1992).

[27] D. M. Ceperley, B. J. Alder, *Phys. Rev. Lett.,* **45,** 566 (1980).

[28] S. J. Clark, M. D. Segall, C. J. Pickard, P. J. Hasnip, M. J. Probert, K. Refson and M. C. Payne, Z. Kristallogr., **220**, 567 (2005).

[29] B. G. Pfrommer, M. Cote, S. G. Louie, M. L. Cohen, *J. Comput. Phys.* **131,** 133 (1997) .

[30] H. J. Monkhorst and J. D. Pack, Phys. Rev., B. **13**, 5188 (1976).

[31] F. Birch, Phys. Rev., **71**, 809 (1974).

[32] J. E. Jaffe, A. Zunger, Phys. Rev., B, **29**, 1882 (1984).

[33] H. Neumann, Phys. Status Solidi (b) **96**, k121 (1986).

[34] L. Roa, J. C. Chervin, J. P. Itié, A. Polian, M. Gauthier, A. Chevy, Physica status solidi (b) **211**,455 (1999).

[35] M. L. Cohen, Phys. Rev., B **32**, 7988 (1985).

[36] V. Milman, , M. C.Warren, , *J. Phys.: Condens. Matter*, **13**, 5585 (2001).

[37] E. Schreiber, O. L. Anderson, and N. Soga, *Elastic Constants and Their Measurement*. McGraw-Hill, New York, 1973.

[38] S. Aydin, M. Simsek, J. Alloys Compod., **509**, 5219 (2011).

[39] A.S. Vermaa, Sheetal Sharma, R. Bhandari, B.K. Sarkar, V.K. Jindal, Mater. Chem. Phys., **132**, 416 (2012).

[40] G. S. Rohrer, *Structure and Bonding in Crystalline Materials*, Cambridge, 2004.

[41] M.D. Segall, R. Shah, C.J. Pickard, M.C. Payne, Phys. Rev., B **54** 16317 (1996).

[42] M.D. Segall, C.J. Pickard, R. Shah, M.C. Payne, Mol. Phys., **89**, 571 (1996).

[43] T. Ouahrani, A. Otero-de-la-Roza, A. H. Reshak, R. Khenata, H. I. Faraoun, B. Amrani, M. Mebrouki, V. Luaña, Physica B **405**, 3658 (2010).